Rapid Communications

Fragile superheavy Fermi liquid in $YbCo_2Zn_{20}$

Y. Shimura,[1,*] T. Kitazawa,[1] S. Tsuda,[1] S. Bachus,[2] Y. Tokiwa,[2] P. Gegenwart,[2] R. Yamamoto,[1] Y. Yamane,[1] I. Nishihara,[1] K. Umeo,[3] T. Onimaru,[1] T. Takabatake,[1] H. T. Hirose,[4] N. Kikugawa,[4] T. Terashima,[4] and S. Uji[4]

[1]*Graduate School of Advanced Sciences of Matter, Hiroshima University, Higashi-Hiroshima 739-8530, Japan*

[2]*Experimental Physics VI, Center for Electronic Correlations and Magnetism, University of Augsburg, D-86159 Augsburg, Germany*

[3]*Cryogenics and Instrumental Analysis Division, N-BARD, Hiroshima University, Higashi-Hiroshima 739-8526, Japan*

[4]*National Institute for Materials Science, Tsukuba, Ibaraki 305-0003, Japan*

(Received 19 May 2019; revised manuscript received 10 May 2020; accepted 11 May 2020; published 1 June 2020)

The cubic Kondo lattice $YbCo_2Zn_{20}$ is one of the heaviest known Fermi liquids. We have measured the low-temperature electrical resistivity $\rho(T)$, magnetic susceptibility $\chi(T)$, and heat capacity $C(T)$ in single crystals of $Yb(Co_{1-x}Ni_x)_2Zn_{20}$ ($x \leqslant 0.126$) and $Yb(Co_{1-x}Fe_y)_2Zn_{20}$ ($y \leqslant 0.07$). While pure $YbCo_2Zn_{20}$ displays maxima in $\rho(T)$ and $\chi(T)$, ascribed to an enhanced crystal electric field (CEF) degeneracy, the maxima are suppressed by small amounts (≈6 at.%) of substitutions of the Co atoms. This goes along with a suppression of superheavy Fermi liquid behavior as manifested in the divergence of C/T. We ascribe the observations to local distortions at the Yb site due to the chemical disorder in the environment, rather than to a chemical pressure effect. This fragileness to the local distortion indicates that superheavy Fermion behavior in $YbCo_2Zn_{20}$ is closely linked to an enhanced CEF degeneracy.

DOI: 10.1103/PhysRevB.101.241102

The effective mass of electrons in metals is a proper index of the strength of the correlation between electrons. In Landau Fermi-liquid theory, the effective mass is proportional to the electronic specific heat coefficient γ and the Pauli paramagnetic susceptibility [1].

Ce- and Yb-based heavy fermion compounds often exhibit a large γ exceeding 1 J/(K^{2}mol). The attraction of such a massive electron has led researchers to the detailed study including doping and magnetic field effects [2–5]. It was found that some Yb-based heavy fermion compounds such as YbBiPt and $YbPt_2X$ (X = Sn, In) exhibit giant γ values close to 10 J/(K^{2}mol) inside the short- and/or long-range magnetic ordered phases [6,7].

$YbCo_2Zn_{20}$ has a paramagnetic ground state with $\gamma \sim$ 8 J/(K^2 mol), which is one order of magnitude larger than those in other members $YbTr_2Zn_{20}$ (Tr = Fe, Ru, Os, Rh, and Ir) of this family with the cubic $CeCr_2Al_{20}$-type structure [8]. Because of this giant γ, $YbCo_2Zn_{20}$ is referred to as a "superheavy" electron system [9].

A naive interpretation of the giant γ may be a manifestation of the weak Kondo effect. Indeed, the electrical resistivity of $YbCo_2Zn_{20}$ shows a coherence peak at $T_H = 2.5$ K [8]. The AC-DC magnetic susceptibility exhibits a maximum at a lower temperature of $T_L = 0.3$ K [10,11]. The temperature-dependent Hall coefficient $R_H(T)$ exhibits two peaks at $T_H =$ 2.5 K and $T_L = 0.3$ K [11]. Emergence of the maximum in the magnetic susceptibility supports that the superheavy Fermi liquid is not formed only by a ground doublet for Yb^{3+} but by crystalline-electric-field (CEF) levels including excited states [12]. The crossover from a localized state to the superheavy fermion state on cooling below 0.2 K is also indicated by a decrease of the ^{59}Co nuclear quadrupole resonance (NQR) frequency [13].

From the analysis of specific heat and magnetization, the energy of the total CEF splitting was estimated to be 30 K with the small splitting of 6–9 K between the ground Γ_6 doublet and the first-excited Γ_8 quartet [14]. This small splitting was observed at 0.6 meV in the neutron inelastic scattering experiments [15]. The two characteristic temperatures of $T_L = 0.3$ K and $T_H = 2.5$ K were explained by the Kondo effect including the contribution of the CEF excited states. T_H is described as $(\Delta_1\Delta_2T_L)^{1/3}$, where Δ_1 and Δ_2 are CEF split energies from the ground state to first and second excited states, respectively [11,16]. For $YbCo_2Zn_{20}$, a large number of $4f$ degeneracy $N = 4$ was inferred from the Grand-Kadowaki-Wood relation, suggesting the coupling of the CEF excited state with conduction electrons [8,17]. Theoretically, the contribution of the CEF excited state to the giant γ in $YbCo_2Zn_{20}$ was also pointed out [18]. Thus, even when the CEF splitting energy of 6–9 K is larger than $T_L = 0.3$ K, the contribution to the superheavy Fermi liquid cannot be ignored.

Among Ce-based heavy-fermion compounds, $CeNi_9Ge_4$ with $\gamma = 5.5$ J/(K^{2}mol) has been established as a rare example with a quasidegenerated CEF ground state [2]. The non-Fermi-liquid behavior observed in $(Ce,La)Ni_9Ge_4$ was explained by taking account of the interplay between a single-site Kondo effect and slightly splitted CEF levels [19]. In particular, the deviation of $C(T)/T$ from the log-T behavior was understood by the crossover from an incoherent Kondo state of quasidegenerated two doublets to a conventional Kondo state for a doublet ground state.

The weak Kondo effect of $YbCo_2Zn_{20}$ may place this compound in the vicinity of the quantum critical point (QCP)

*simu@hiroshima-u.ac.jp

close to a magnetically ordered phase. In fact, application of pressures 1.0–1.8 GPa induces an antiferromagnetic order at ≈0.2 K [11,20]. This critical pressure P_c of $YbCo_2Zn_{20}$ is smaller than that of the isostructural $YbIr_2Zn_{20}$ (P_c = 5.2 GPa) and $YbFe_2Zn_{20}$ (P_c = 18.2 GPa), indicating the closeness of $YbCo_2Zn_{20}$ to the QCP [21,22].

In spite of the cubic structure, $YbCo_2Zn_{20}$ shows strong magnetic anisotropy [11,14,23]. Notably, applying magnetic fields of $B \geqq 6$ T parallel to the [111] direction crosses the two CEF levels, resulting in a long-range ordered phase [14,24]. As the order parameters, Γ_3-type antiferro-quadrupole moments were proposed from the simulation of magnetization and specific heat based on the mean-field theory. The emergence of the elastic softening on cooling down to ≈1 K also suggests that quadrupole degrees of freedom of quasidegenerated CEF levels become active at low temperatures [25].

Application of B || [100], on the other hand, readily lifts the ground doublet [14]. This strong Zeeman effect on the ground doublet results in the quenching of the heavy effective mass by ≈1/100 and the suppression of the magnetic entropy [10]. This suppression of entropy by increasing the magnetic field to 8 T is useful for the adiabatic demagnetization cooling, as was proposed from the study of the low-temperature magnetocaloric effect [9].

The chemical dope effect has been well studied in $Yb(Fe_yCo_{1-y})_2Zn_{20}$ ($0 \leqq y \leqq 1$) [26]. The coherence peak in the resistivity for $y = 1$ at $T_{\rho\max} \approx 40$ K is suppressed by Co substitution and disappears in the range $0.1 \leqq y \leqq 0.6$. It reappears near the Co side of $y \leqq 0.1$, again. Thus, the Fe substitution effect in $YbCo_2Zn_{20}$ cannot be understood by the increase of T_K induced by hole doping. Therefore, it is necessary to compare the effects of electron (Ni) and hole (Fe) doping on the superheavy Fermi liquid, probably coupled with the quasidegenerated CEF ground state.

Single-crystalline samples of $Yb(Co_{1-x}Ni_x)_2Zn_{20}$ ($x \leqq 0.126$) and $Yb(Co_{1-y}Fe_y)_2Zn_{20}$ ($y = 0.070$) were grown by the Zn-self-flux method [8]. The crystals have a triangular surface approximately 5 mm in diameter. The atomic compositions are determined by wavelength dispersive electron-probe microanalysis (EPMA). The actual values x are about 1/3 of the initial ones. The cubic $CeCr_2Al_{20}$-type crystal structure was confirmed by powder x-ray diffraction analysis. The Rieldvelt analysis showed that the lattice parameter decreases only by 0.05% with increasing x to 0.126.

DC magnetic susceptibility for $T > 1.9$ K was measured in a commercial superconducting quantum interference device (SQUID) magnetometer (Quantum Design, MPMS). AC magnetic susceptibility at temperatures down to 0.024 K was measured by using a top-loading dilution refrigerator at Tsukuba Magnet Laboratory, NIMS. The amplitude and frequency of the modulated field are 3.7 gauss and 67.2 Hz, respectively. Both the modulated and the static DC field were applied along the [110] direction.

The electrical resistivity was measured in a wide temperature range between 0.04 and 300 K by using an adiabatic demagnetization refrigerator (ADR, mF-ADR50) and a commercial physical properties measurement system (Quantum Design, PPMS) with an ADR option. Specific heat measurements for $T > 0.4$ K were performed in the commercial calorimeter (PPMS) by the relaxation method. Specific heat

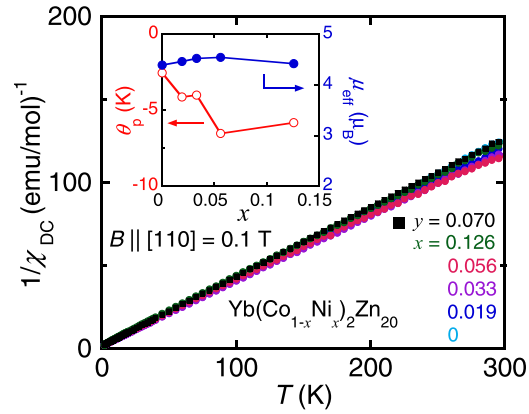

FIG. 1. The inverse DC magnetic susceptibility χ_{DC}^{-1} for B || [110] in $Yb(Co_{1-x}Ni_x)_2Zn_{20}$ and $Yb(Co_{1-y}Fe_y)_2Zn_{20}$. The inset shows the x dependence of the paramagnetic Curie temperatures and the effective magnetic moments.

at lower temperatures down to 0.07 K was measured by the quasiadiabatic heat pulse method using a laboratory-made calorimeter installed in the dilution refrigerator of University of Augsburg.

Figure 1 shows the temperature dependence of the inverse DC magnetic susceptibility $\chi_{DC}^{-1}(T)$ for B || [110] = 0.1 T. The inset shows the x dependence of the effective moment μ_{eff} and the paramagnetic Curie temperature θ_p obtained from the Curie-Weiss fit to the data of $\chi_{DC}^{-1}(T)$ for 10 K < T < 300 K. μ_{eff} and θ_p in $Yb(Co_{1-y}Fe_y)_2Zn_{20}$ ($y = 0.070$) are 4.38 μ_B and −4.1 K, respectively. All the values of μ_{eff} are close to 4.54 μ_B expected for the free Yb^{3+} ion, indicating no change in the valence of Yb^{3+} ion.

Figure 2 shows the low-temperature data of $\chi_{AC}(T)$ at 0.2 T. In the Supplemental Material [27], we show $\chi_{AC}(T)$ at zero DC field. The upturn below ≈0.07 K is probably due to a magnetic impurity because similar upturns were observed in all samples including the nondoped sample [27]. In order

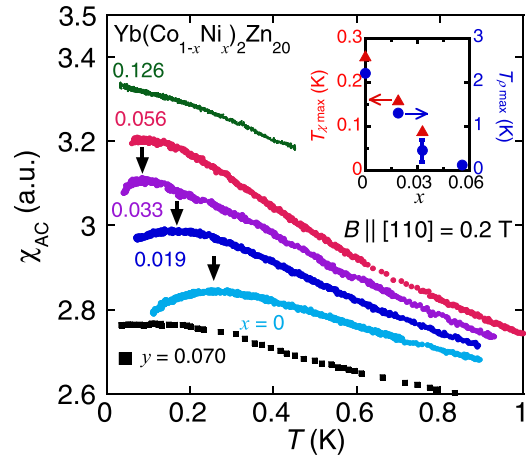

FIG. 2. Temperature dependence of the AC magnetic susceptibility $\chi_{AC}(T)$ in $Yb(Co_{1-x}Ni_x)_2Zn_{20}$ and $Yb(Co_{1-y}Fe_y)_2Zn_{20}$ ($y = 0.070$) for B || [110] = 0.2 T at temperatures down to 0.024 K. All the data are vertically shifted for clarify. The inset shows $T_{\chi max}$ in the AC magnetic susceptibility (left) and $T_{\rho max}$ in the electrical resistivity (right) obtained from Fig. 3 as a function of x.

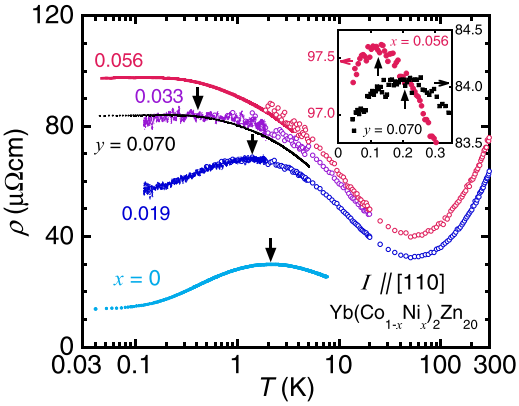

FIG. 3. Temperature dependence of the resistivity $\rho(T)$ of $Yb(Co_{1-x}Ni_x)_2Zn_{20}$ and $Yb(Co_{1-y}Fe_y)_2Zn_{20}$ ($y = 0.070$) for the current I || [110] from 300 to 0.04 K. The inset represents the low-temperature data of $\rho(T)$ for $x = 0.056$ and $y = 0.070$ showing a maximum at 0.12 and 0.2 K, respectively.

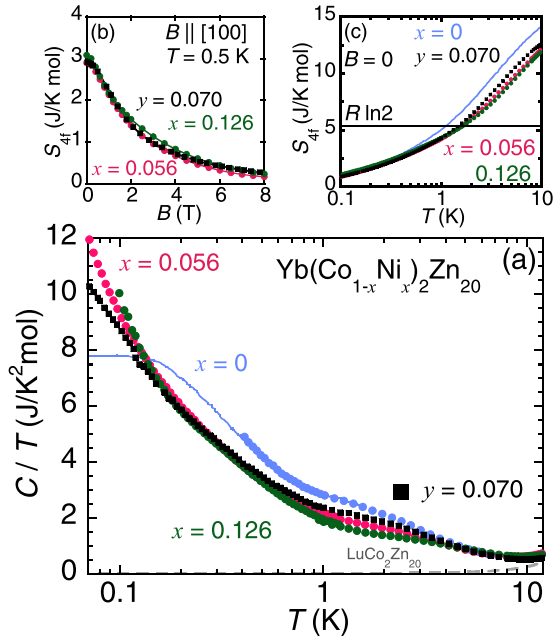

FIG. 4. (a) Temperature dependence of the specific heat divided by temperature, C/T, for $Yb(Co_{1-x}Ni_x)_2Zn_{20}$ with $x = 0$, 0.056, 0.126 and $Yb(Co_{1-y}Fe_y)_2Zn_{20}$ ($y = 0.070$) in zero field. The solid and the broken lines show the data of $YbCo_2Zn_{20}$ and $LuCo_2Zn_{20}$ referred from Ref. [14], respectively. (b) Field dependence of the magnetic entropy of $4f$ electrons $S_{4f}(B)$ at 0.5 K for B || [100]. (c) Temperature dependence of the magnetic entropy of $4f$ electrons $S_{4f}(T)$ at zero field.

to suppress the divergence of $\chi_{AC}(T)$, a DC field of B || [110] = 0.2 T was applied. For $x = 0$, $\chi_{AC}(T)$ in Fig. 2 exhibits a broad peak at 0.27 K in accordance with the previous $\chi_{DC}(T)$ data measured at 0.3 T [11]. With increasing x, this peak monotonically shifts to lower temperatures. At $x = 0.056$ and $y = 0.070$, such a broad peak is not seen down to the lowest temperature of 0.04 K.

Figure 3 represents the semilogarithmic plot of the temperature dependence of $\rho(T)$ in $Yb(Co_{1-x}Ni_x)_2Zn_{20}$ and $Yb(Co_{1-y}Fe_y)_2Zn_{20}$ ($y = 0.070$) from 300 to 0.04 K. All the data exhibit $-\log T$ dependence below $\approx$40 K due to the Kondo effect followed by a broad maximum at temperatures below 3 K, as indicated by the arrows. With increasing x and y, the residual resistivity is enhanced and the broad peak monotonically shifts to lower temperatures. As for $y = 0.070$, this behavior is consistent with the previous result [26]. For $x = 0.056$ and $y = 0.070$, maximum can be seen in the expanded scale as shown in the inset of Fig. 3. In the inset of Fig. 2, we represent the x dependence of $T_{\rho max}$ and $T_{\chi max}$, determined from broad peaks in $\rho(T)$ and $\chi_{AC}(T)$ in the inset of Fig. 2, respectively. Both temperatures monotonically approach absolute zero at around $x = 0.056$.

A similar suppression of $T_{\rho max}$ has been reported for various doped $YbCo_2Zn_{20}$ systems [9,26,28]. We first discuss the case of Fe-doped $YbCo_2Zn_{20}$ [26]. It was expected that $T_{\rho max}$ continuously increases with increasing Fe concentration in $Yb(Co_{1-y}Fe_y)_2Zn_{20}$ because $YbFe_2Zn_{20}$ has $T_{\rho max} \sim 40$ K much higher than 2.5 K for $YbCo_2Zn_{20}$ [29]. However, the temperature dependence of $\rho(T)$ for $0 \leqq y \leqq 0.125$ is rather similar to that found in $Yb(Co_{1-x}Ni_x)_2Zn_{20}$ in our paper. For example, $T_{\rho max}$ for $y = 0.043$ is suppressed to below 0.4 K as found for $x = 0.033$ [26].

This decrease in $T_{\rho max}$ with substitution is in common with $(Yb,Sc)Co_2Zn_{20}$, $YbCo_2(Zn,Cd)_{20}$, and $YbCo_2(Zn,Cu)_{20}$ [9,28]. Thus, generally the Kondo lattice coherence in $YbCo_2Zn_{20}$ can easily be broken by any chemical doping, irrespective of the doped sites. These results suggest that the atomic disorder effect on the ground-state properties in $YbCo_2Zn_{20}$ dominates over chemical pressure or carrier doping. The large enhancement of the residual resistivity as shown in Fig. 3 can also be attributed to the strong scattering of the correlated electrons by the atomic disorder.

The chemical pressure effect can be ignored because the volume decrease at $x = 0.126$ is as small as 0.05% with respect to that for $x = 0$. On the other hand, applying pressure of 1.8 GPa leads to a quantum critical point, and a long-range antiferromagnetic order appears at 0.3 K under 3 GPa [11]. Using the critical pressure $P_c = 1.8$ GPa and the bulk modulus $C_B = 80$ GPa, we estimate the lattice parameter change necessary to induce the magnetic order [25]. The bulk modulus is described as $C_B = -V\Delta P/\Delta V \sim -L^3\Delta P/(3L^2\Delta L) = -L\Delta P/(3\Delta L)$, where V and L are the unit-cell volume and the lattice parameter of the cubic structure, respectively. From this relation, we obtain ΔL as -0.105 Å. This compression at the pressure-tuned magnetic quantum critical point is one order of magnitude larger than the actual decrease in the lattice parameter for $x = 0.126$, as $L(x = 0) - L(x = 0.126) = -0.007$ Å. Therefore, the suppression of $T_{\rho max}$ and $T_{\chi max}$ in $Yb(Co_{1-x}Ni_x)_2Zn_{20}$ at $x \sim 0.1$ cannot be explained by approaching a quantum critical point which is induced by the isotropic lattice shrinkage (i.e., hydrostatic pressure effect). Thus, we conjecture that the superheavy Fermi liquid in $YbCo_2Zn_{20}$ is fragile to the atomic disorder.

Figure 4(a) shows the temperature dependence of the specific heat divided by temperature $C(T)/T$ in $Yb(Co_{1-x}Ni_x)_2Zn_{20}$ with $x = 0, 0.056, 0.126$ and $Yb(Co_{1-y}Fe_y)_2Zn_{20}$ ($y = 0.070$). We also plot the reported data of $YbCo_2Zn_{20}$ (solid line) and the nonmagnetic reference

$LuCo_2Zn_{20}$ (broken line) from Ref. [14]. Our C/T data for $x = 0$ overlap with the reported ones in the temperature range between 0.4 and 15 K. In addition, C/T of $LuCo_2Zn_{20}$ is very small for $T < 5$ K, compared with that of Yb-based samples. Upon cooling below 1 K, the C/T data for $x = 0.056$, 0.126 and $y = 0.070$ are strongly enhanced toward divergence. The value of C/T at the base temperature of 0.07 K approaches 10–12 J/(K^2 mol), which is significantly enhanced, compared to 8 J/(K^2 mol) for $x = 0$. The divergent behavior of C/T down to lowest temperatures indicates that the superheavy Fermi liquid in $YbCo_2Zn_{20}$ is sensitive to the tiny amount of chemical doping. Above 0.2 K, the values of C/T for the Ni- and Fe-doped systems become smaller than that for $x = 0$.

As noted in the introduction, $YbFe_2Zn_{20}$ is a paramagnetic heavy fermion system with a higher $T_K(T_{\rho\max} \sim 40$ K) than that in $YbCo_2Zn_{20}$. Therefore, the suppression of the Fermi-liquid behavior induced by the Fe substitution for Co rules out the scenarios connected with a magnetic ordered phase. As the scenarios, we conceive of the magnetic quantum criticality preserving the itineracy of f electrons or localization of f electrons by eliminating the c-f hybridzation (Kondo breakdown) [30,31]. Since chemical doping inevitably induces randomness in the magnetic interaction, it would be possible that the magnetic moments are randomly frozen or that clusters of magnetic moments show a slow relaxation in the so-called Griffiths phase [32]. These "magnetic" origins are also ruled out. The similarity of C/T, χ_{AC}, and ρ between the Fe- and Ni-doped systems requires a different scenario. Non-Fermi-liquid behavior induced by chemical substitution is often explained by the Kondo disorder model [33]. This model predicts a linear decrease of $\rho(T)$ on cooling [33,34]. However, such a decrease of $\rho(T)$ is not observed for $x = 0.056$ and $y = 0.070$ with a broad maximum at 0.1–0.2 K.

In both Fe- and Ni-doped systems, C/T divergently increases on cooling, especially following $-\log T$ below 0.2 K. In contrast, $\chi(T)$ tends to saturate as temperature goes to zero. These characteristic behaviors of C/T and $\chi(T)$ resemble those in (Ce,La)Ni_9Ge_4 with a quasidegenerated CEF ground state [2]. These temperature dependences are theoretically explained by the interplay between the Kondo effect and the quasidegenerate CEF ground state [19,35]. Similar behaviors have been observed also in the electron-doped $Ce(Ni_{0.8}Cu_{0.2})_9Ge_4$ and hole-doped $Ce(Ni_{0.9}Co_{0.1})_9Ge_4$ [36,37], which correspond to Yb(Co, T)$_2Zn_{20}$ with T = Ni and Fe, respectively.

As for the energy distribution of the CEF levels of the quasisextet ground state of Yb^{3+} in doped samples, we consider it as follows: If the low-lying quartet (two Kramers doublets) is randomly distributed in energy, the Schottky peak in C/T due to the excitation from the doublet ground state to the low-lying quartet should become broad. Assuming CEF effect solely, distribution of CEF levels should make the positive slope in C/T around $T = 0$ higher, compared with that for the nondoped system. This is opposite to the negative slope of C/T as observed for $x = 0.056$ and $y = 0.07$. Therefore, the distribution of the quasidegenerated CEF ground state does not explain the divergent C/T in the doped samples.

A common effect of doping into $CeNi_9Ge_4$ and $YbCo_2Zn_{20}$ is the suppression of coherence of the Kondo lattice induced by atomic disorder. Indeed, the Kondo coherence observed in $\rho(T)$ on cooling below $T_{\rho\max}$ is suppressed in both Ce(Ni, T)$_9Ge_4$ (T = Co and Cu) and Yb(Co, T)$_2Zn_{20}$ (T = Ni and Fe).

Now, let us discuss the degeneracy of the ground state from the magnetic entropy of the $4f$ electrons S_{4f} in $Yb(Co_{1-x}Ni_x)_2Zn_{20}$ and $Yb(Co_{0.930}Fe_{0.070})_2Zn_{20}$. In principle, S_{4f} can be calculated by integrating the C/T data from $T = 0$ to $T = T$ after subtracting that of $LuCo_2Zn_{20}$. We performed a thorough thermodynamic study to obtain the absolute value of S_{4f}. For heavy-fermion systems, one assumes that C/T becomes constant as T goes to zero. This is valid for $x = 0$ with the Fermi-liquid ground state. However, this assumption is not correct for $x = 0.056$ and 0.126 for which C/T diverges on cooling to the lowest measured temperature. In this work, we evaluated the absolute value of S_{4f} at 0.5 K from independent measurements of the field dependence of $C(B)$ and the magnetic Grüneisen ratio $\Gamma_H = T^{-1}(dT/dB)_S$ up to 8 T at 0.5 K for B || [100]. The details of the calculation is given in the Supplemental Material [27]. We determined Γ_H by measuring the magnetocaloric effect under the quasiadiabatic conditions [38]. We also used temperature dependence of C/T at 8 T, where the $4f$ magnetic entropy is quenched below 1 K because of the Zeeman splitting of the CEF levels. Figure 4(b) displays field dependence of S_{4f} at 0.5 K, obtained from $C(T)/T$ at 8 T and $C(B)$ and $\Gamma_H(B)$ at 0.5 K (see the Supplemental Material [27]). In this method, the absolute values of the entropy at 0.5 K in zero field are evaluated to be 2.90, 3.08, and 2.91 J/(K mol) for $x = 0.056$, 0.126, and $y = 0.070$, respectively. The entropy curves in Fig. 4(c) are obtained by shifting the temperature dependence of the relative entropy change ΔS_{4f} to agree with the absolute values at 0.5 K. It is noteworthy that S_{4f} for $x = 0.056$ and 0.126 and $y = 0.070$ for $T > 1$ K are significantly smaller than that for $x = 0$.

As noted in the introduction, one of the important characters of cubic $YbCo_2Zn_{20}$ is that the first-excited CEF state of Γ_8 quartet is close to the Γ_6 ground doublet, whose splitting energy is 6−9 K [14,24]. The Γ_8 quartet, and the quasisextet including Γ_8, are not protected by the time-reversal symmetry. Therefore, the degeneracy is readily lifted by the breaking of the local symmetry of the Yb site which is a result from the atomic substitution. Such an effect more clearly appears in a nonmagnetic ground state of the non-Kramers systems like Pr-based PrT_2X_{20} [39,40]. Since the Yb^{3+} ion is a Kramers ion, the degeneracy of the ground doublet with $S_{4f} = R\ln 2$ cannot be removed by the local disorder. Based on this idea, it can be naturally understood that the difference in the S_{4f} between $x = 0$ and 0.056 becomes clear above $R\ln 2$ for $T >$ 1 K as shown in Fig. 4(c).

As remarked by Torikachvili *et al.*, the superheavy fermion state in $YbCo_2Zn_{20}$ cannot be explained by considering solely the subspace of the Kramers doublet ground state, but the contribution of the CEF excited state needs to be taken into account [8]. The fact that the suppression of S_{4f} by the chemical doping, irrespective of the doped sites, manifests that the high degrees of freedom in the quasisextet ground state is indispensable for the formation of the superheavy Fermi liquid in $YbCo_2Zn_{20}$.

In summary, we reported the DC-AC magnetic susceptibility, electrical resistivity, and specific heat of

$Yb(Co_{1-x}Ni_x)_2Zn_{20}$ ($x \leqslant 0.126$) and $Yb(Co_{0.930}Fe_{0.070})_2Zn_{20}$ at temperatures down to 0.024 K. By increasing the Ni content x to 0.056, $T_{\rho\max}$ and $T_{\chi\max}$ monotonically decrease and approach zero. In contrast to the weak temperature dependence in ρ and χ, C/T exhibits a divergent increase on cooling down to 0.07 K, where the value of C/T exceeds 10 $J/(K^2\,mol)$. The similar effect of Ni and Fe doping suggests that the superheavy Fermi liquid in $YbCo_2Zn_{20}$ is fragile to the atomic disorder by substitution. This fact fully supports the model that the highly quasidegenerated CEF ground state, which is easily broken by the disorder, is necessary for the formation of the superheavy Fermi liquid.

Electron-probe microanalysis, DC magnetization, and electrical resistivity measurements were performed at the Cryogenics and Instrumental Analysis Division, N-BARD, Hiroshima University. Part of this work was supported by the NIMS Joint Research Hub Program. This work was financially supported by the Iketani Science and Technology Foundation (Grant No. 0301080-A) and JSPS KAKENHI Grants No. JP15H05886, No. JP18KK0078, and No. JP18H01182.

[1] A. C. Hewson, *The Kondo Problem to Heavy Fermions* (Cambridge University Press, Cambridge, UK, 1993).
[2] U. Killer, E.-W. Scheidt, G. Eickerling, H. Michor, J. Sereni, T. Pruschke, and S. Kehrein, Phys. Rev. Lett. **93**, 216404 (2004).
[3] C. Gold, P. Gross, L. Peyker, G. Eickerling, G. G. Simeoni, O. Stockert, E. Kampert, F. Wolff-Fabris, H. Michor, and E.-W. Scheidt, J. Phys.: Condens. Matter **24**, 355601 (2012).
[4] E. D. Mun, S. L. Bud'ko, C. Martin, H. Kim, M. A. Tanatar, J.-H. Park, T. Murphy, G. M. Schmiedeshoff, N. Dilley, R. Prozorov, and P. C. Canfield, Phys. Rev. B **87**, 075120 (2013).
[5] J. Lee, A. Rabus, C. Coutts, and E. Mun, Phys. Rev. B **99**, 045135 (2019).
[6] T. Gruner, D. Jang, A. Steppke, M. Brando, F. Ritter, C. Krellner, and C. Geibel, J. Phys.: Condens. Matter **26**, 485002 (2014).
[7] Z. Fisk, P. C. Canfield, W. P. Beyermann, J. D. Thompson, M. F. Hundley, H. R. Ott, E. Felder, M. B. Maple, M. A. Lopez de la Torre, P. Visani, and C. L. Seaman, Phys. Rev. Lett. **67**, 3310 (1991).
[8] M. S. Torikachvili, S. Jia, E. D. Mun, S. T. Hannahs, R. C. Black, W. K. Neils, D. Martien, S. L. Bud'ko, and P. C. Canfield, Proc. Natl. Acad. Sci. USA **104**, 9960 (2007).
[9] Y. Tokiwa, B. Piening, H. S. Jeevan, S. L. Bud'ko, P. C. Canfield, and P. Gegenwart, Sci. Adv. **2**, e1600835 (2016).
[10] M. Ohya, M. Matsushita, S. Yoshiuchi, T. Takeuchi, F. Honda, R. Settai, T. Tanaka, Y. Kubo, and Y. Ōnuki, J. Phys. Soc. Jpn. **79**, 083601 (2010).
[11] F. Honda, Y. Taga, Y. Hirose, S. Yoshiuchi, Y. Tomooka, M. Ohya, J. Sakaguchi, T. Takeuchi, R. Settai, Y. Shimura, T. Sakakibara, I. Sheikin, T. Tanaka, Y. Kubo, and Y. Ōnuki, J. Phys. Soc. Jpn. **83**, 044703 (2014).
[12] V. T. Rajan, Phys. Rev. Lett. **51**, 308 (1983).
[13] T. Mito, H. Hara, T. Ishida, K. Nakagawara, T. Koyama, K. Ueda, T. Kohara, K. Ishida, K. Matsubayashi, Y. Saiga, and Y. Uwatoko, J. Phys. Soc. Jpn. **82**, 103704 (2013).
[14] T. Takeuchi, S. Yoshiuchi, M. Ohya, Y. Taga, Y. Hirose, K. Sugiyama, F. Honda, M. Hagiwara, K. Kindo, R. Settai, and Y. Ōnuki, J. Phys. Soc. Jpn. **80**, 114703 (2011).
[15] K. Kaneko, S. Yoshiuchi, T. Takeuchi, F. Honda, R. Settai, and Y. Ōnuki, J. Phys.: Conf. Ser. **391**, 012026 (2012).
[16] K. Yamada, K. Yosida, and K. Hanzawa, Prog. Theor. Phys. **71**, 450 (1984).
[17] N. Tsujii, H. Kontani, and K. Yoshimura, Phys. Rev. Lett. **94**, 057201 (2005).
[18] M. A. Romero, A. A. Aligia, J. G. Sereni, and G. Nieva, J. Phys.: Condens. Matter **26**, 025602 (2014).
[19] F. B. Anders and T. Pruschke, Phys. Rev. Lett. **96**, 086404 (2006).
[20] Y. Saiga, K. Matsubayashi, T. Fujiwara, M. Kosaka, S. Katano, M. Hedo, T. Matsumoto, and Y. Uwatoko, J. Phys. Soc. Jpn. **77**, 053710 (2008).
[21] F. Honda, S. Yasui, S. Yoshiuchi, T. Takeuchi, R. Settai, and Y. Ōnuki, J. Phys. Soc. Jpn. **79**, 083709 (2010).
[22] U. S. Kaluarachchi, L. Xiang, J. Ying, T. Kong, V. Struzhkin, A. Gavriliuk, S. L. Bud'ko, and P. C. Canfield, Phys. Rev. B **98**, 174405 (2018).
[23] Y. Shimura, T. Sakakibara, S. Yoshiuchi, F. Honda, R. Settai, and Y. Ōnuki, J. Phys.: Conf. Ser. **391**, 012066 (2012).
[24] Y. Shimura, T. Sakakibara, S. Yoshiuchi, F. Honda, R. Settai, and Y. Ōnuki, J. Phys. Soc. Jpn. **80**, 073707 (2011).
[25] Y. Nakanishi, T. Fujino, K. Ito, M. Nakamura, M. Yoshizawa, Y. Saiga, M. Kosaka, and Y. Uwatoko, Phys. Rev. B **80**, 184418 (2009).
[26] T. Kong, V. Taufour, S. L. Bud'ko, and P. C. Canfield, Phys. Rev. B **95**, 155103 (2017).
[27] See Supplemental Material at http://link.aps.org/supplemental/10.1103/PhysRevB.101.241102 for the specific heat and the magnetic Grüneisen ratio under magnetic field in addition to the AC magnetic susceptibility at zero DC field, which includes Refs. [14,38].
[28] R. Kobayashi, H. Takamura, Y. Higa, Y. Ikeda, K. Matsubayashi, Y. Uwatoko, H. Yoshizawa, and N. Aso, J. Phys.: Conf. Ser. **807**, 012009 (2017).
[29] S. K. Kim, M. S. Torikachvili, S. L. Bud'ko, and P. C. Canfield, Phys. Rev. B **88**, 045116 (2013).
[30] T. Moriya and T. Takimoto, J. Phys. Soc. Jpn. **64**, 960 (1995).
[31] Q. Si, S. Rabello, K. Ingersent, and J. L. Smith, Nature (London) **413**, 804 (2001).
[32] A. H. Castro Neto, G. Castilla, and B. A. Jones, Phys. Rev. Lett. **81**, 3531 (1998).
[33] E. Miranda, V. Dobrosavljević, and G. Kotliar, Phys. Rev. Lett. **78**, 290 (1997).

[34] D. Gnida, Phys. Rev. B **97**, 081112(R) (2018).
[35] H.-U. Desgranges, Phys. B: Condens. Matter **473**, 93 (2015).
[36] L. Peyker, C. Gold, W. Scherer, H. Michor, and E.-W. Scheidt, J. Phys.: Conf. Ser. **273**, 012049 (2011).
[37] L. Peyker, C. Gold, E.-W. Scheidt, W. Scherer, J. G. Donath, P. Gegenwart, F. Mayr, T. Unruh, V. Eyert, E. Bauer, and H. Michor, J. Phys.: Condens. Matter **21**, 235604 (2009).
[38] Y. Tokiwa and P. Gegenwart, Rev. Sci. Instrum. **82**, 013905 (2011).
[39] M. Tsujimoto, Y. Matsumoto, and S. Nakatsuji, J. Phys.: Conf. Ser. **592**, 012023 (2015).
[40] R. J. Yamada, T. Onimaru, K. Uenishi, Y. Yamane, K. Wakiya, K. T. Matsumoto, K. Umeo, and T. Takabatake, J. Phys. Soc. Jpn. **88**, 054704 (2019).